PASSIVE MECHANICAL PROPERTIES OF HUMAN LEUKOCYTES

GEERT W. SCHMID-SCHÖNBEIN, KUO-LI PAUL SUNG, HÜSNÜ TÖZEREN, RICHARD SKALAK, AND SHU CHIEN, *Department of Physiology, College of Physicians and Surgeons, and Department of Civil Engineering and Engineering Mechanics, Columbia University, New York 10032*

ABSTRACT Micropipette experiments are used to determine the rheological properties of human leukocytes. Individual cells in EDTA are subjected to a known aspiration pressure via a micropipette, and their surface deformation from the undeformed spherical shape is recorded on a television monitor. The cells are mathematically modeled as homogeneous spheres, and a standard solid viscoelastic model is found to describe accurately the deformation of the cell for small strains. These experimental and theoretical studies provide the basis for further investigations of leukocyte rheology in health and disease.

INTRODUCTION

Study of the mechanical properties of leukocytes is important for an understanding of their function in the circulation. A rheological model is needed for the analysis of almost every problem in physiology involving the leukocytes, such as the deformation of the leukocytes during release from the bone marrow, their motion and deformation in blood vessels, leukocyte rolling on the venous endothelium, migration through the capillary wall into the interstitium, deformation during phagocytosis, and other phenomena. Once a rheological model is available, each of these phenomena can be analyzed, and a quantitative understanding of the function of leukocytes can be developed.

A convenient and relatively accurate way to test the mechanical properties of single cells is the micropipette experiment, which has been applied frequently to human erythrocytes (Rand and Burton, 1964; Evans, 1973; LaCelle et al., 1977; Chien, 1977) and leukocytes (Lichtman, 1973; Miller and Myers, 1975). Rheological tests have led to the development of the current mechanical model of the erythrocyte as a thin viscoelastic membrane filled with a Newtonian viscous hemoglobin solution. The erythrocyte membrane has been found to have an elastic shear modulus several orders of magnitude lower than the area modulus (Evans and Hochmuth, 1978; Chien et al., 1978).

Recently, morphometric measurements on human leukocytes have been reported (Schmid-Schönbein et al., 1980*b*). In an isotonic salt solution the undeformed leukocyte is roughly spherical and has many convoluted folds on its surface, which provide an excess membrane area (e.g., ~83% in neutrophilic leukocytes) over that needed to enclose its volume as a smooth sphere. During swelling of the leukocyte in a hypotonic salt solution, the membrane

---

Dr. Schmid-Schönbein's present address is the Department of Applied Mechanics and Engineering Sciences, University of California-San Diego, La Jolla, Calif. Dr. Tözeren's current address is the Department of Engineering Sciences, Middle East Technical University, Ankara, Turkey.

unfolds, although the actual membrane area remains constant, within the error of the measurement. In neutrophils the combined volume of the nucleus, granules, and mitochondria occupy ~37% of the cell volume, whereas 63% is occupied by the cytoplasmic matrix; similar values are found in monocytes and eosinophils. The nucleus is segmented and fills ~21% of the cell volume, and it too has an excess membrane area, of ~98%. The electron microscopic studies have also shown that leukocytes have many other membranes besides the plasma and nucleus membrane; e.g., around all granules, in the cell golgi region, and in the endoplasmic reticulum.

Erythrocytes do not undergo deformation unless an external force is applied, although there may be membrane flickering due to Brownian motion. In contrast, when human leukocytes are freely suspended in plasma or Ringer's solution, without the action of an external mechanical force they will spontaneously deform by projecting portions of the cell membrane and cytoplasm out from the main cell body. These projections originate at different points on the cell surface, grow at the rate of ~10 μm/min, and may become several micrometers long. Since the cell deformation is asymmetric, the required force cannot be due only to Brownian motion. The motion is spontaneous and the mechanical energy needed for deformation is supplied by the cell itself. We say that the cell is now in an active state (Schmid-Schönbein et al., 1981). If the leukocytes are suspended in a medium with EDTA, they remain essentially spherical for several hours, but after 7–8 h they will again exhibit spontaneous deformations. There are other chemical agents, such as cytochalasin B, which can eliminate the spontaneous deformations of the leukocytes.

In contrast to the active state, we refer to the leukocytes not undergoing spontaneous deformation as being in a passive state with passive mechanical properties. In the passive state the leukocytes deform only in response to an externally applies stress, such as an adhesive stress or the aspiration pressure of a micropipette. In this study we report first on the passive properties of human neutrophils in the presence of EDTA. The cell deformation in response to a well defined stress field applied via a micropipette was monitored through a light microscope with a high resolution. To analyze the time-dependent deformation of the neutrophil in these experimental studies, a viscoelastic model has been derived in which the leukocyte is treated as a homogeneous viscoelastic solid sphere. This study of the passive properties is of interest because in the microcirculation leukocytes are often observed without the occurrence of spontaneous deformation (Bagge and Brånemark, 1977; Schmid-Schönbein et al., 1980*a*). The leukocytes in the arterioles are usually spherical. They may be deformed as they traverse the capillaries, but in the venules they return to the spherical shape (Bagge and Brånemark, 1977). It is probably a reasonable approximation to consider only the passive viscoelastic properties in problems of the flow of leukocytes in a single file capillary (Tözeren and Skalak, 1978) or during their rolling on the endothelium. On the other hand, leukocyte migration across the endothelium or in a chemotactic gradient (Gallin and Quie, 1978) or during phagocytosis (Elsbach, 1974) can only be described if the active properties are considered as well.

A CONTINUUM THEORY FOR LEUKOCYTES

In the following we consider the leukocyte to be a solid homogeneous viscoelastic body. In the undeformed state the cell is spherical, and we neglect the surface foldings. The model of a

smooth homogeneous sphere must be regarded as only an approximate model because in fact the interior of the cell is not homogeneous and the surface is not smooth. Neglecting the presence of the membrane is probably not a serious error because such a wrinkled membrane can impart very little stress until it is stretched smooth.

Using index notation, let σ_{ij} be the stress inside the leukocyte (see, e.g., Fung, 1965, for notational conventions). Each component of σ_{ij} is regarded as function of the three cartesian coordinates (x_1, x_2, x_3) and time. The stress deviator σ'_{ij} is defined as

$$\sigma'_{ij} = \sigma_{ij} - \tfrac{1}{3}\,\sigma_{kk}\delta_{ij}, \tag{1}$$

where δ_{ij} is the Kronecker symbol, and a double index indicates a summation, i.e., $\sigma_{kk} = \sigma_{11} + \sigma_{22} + \sigma_{33}$. The hydrostatic pressure p is equal to $(-\tfrac{1}{3})\sigma_{kk}$. Let $u_i(x_1, x_2, x_3, t)$ be the displacement inside the cell with respect to the coordinates x_i in the deformed state. Then the Eulerian strain is defined as

$$e_{ij} = \frac{1}{2}\left(\frac{\partial u_i}{\partial x_j} + \frac{\partial u_j}{\partial x_i} - \frac{\partial u_k \partial u_k}{\partial x_i \partial x_j}\right).$$

If the displacement gradients during deformation are small, then the strain-displacement relationship may be approximated in the usual form:

$$e_{ij} = \frac{1}{2}\left(\frac{\partial u_i}{\partial x_j} + \frac{\partial u_j}{\partial x_i}\right). \tag{2}$$

The strain deviator for e_{ij} is defined as

$$e'_{ij} = e_{ij} - \tfrac{1}{3}\,\delta_{ij} e_{kk}. \tag{3}$$

The leukocyte, similar to other soft biological tissues, contains a high proportion of water, and may therefore be assumed to have constant density at the relatively low stresses that are applied to its surface and in the absence of water filtration across its membrane. In this case the condition of conservation of mass reduces to the equation (Fung, 1965)

$$e_{kk} = \frac{\partial u_k}{\partial x_k} = 0. \tag{4}$$

Therefore,

$$e'_{ij} = e_{ij}. \tag{5}$$

When a leukocyte is freely suspended in a salt solution, its density is almost equal to the density of the water medium. In this experiment, therefore, all body forces acting on the cell, such as the gravitational force or inertial force, are negligible in comparison with the force applied by the suction pressure. The equation of equilibrium in the absence of body forces reduces to

$$\frac{\partial \sigma_{ij}}{\partial x_j} = 0, \tag{6a}$$

or, in terms of the stress deviator,

$$\frac{\partial \sigma'_{ij}}{\partial x_j} = \frac{\partial p}{\partial x_i}. \tag{6b}$$

Next we need a relationship between σ'_{ij} and e'_{ij}. In general, leukocytes exhibit viscoelastic properties. In the micropipette experiment these will be tested by means of a creep experiment. As will be discussed below, the essential features of the deformation history for small displacements can be approximated by a standard solid viscoelastic model (Fig. 1) with the following constitutive equation:

$$\sigma'_{ij} + \frac{\mu}{k_2}\dot{\sigma}'_{ij} = e'_{ij}k_1 + \dot{e}'_{ij}\,\mu\left(1 + \frac{k_1}{k_2}\right). \tag{7}$$

In this equation k_1 and k_2 represent two elastic coefficients measured in dyn/cm^2, and μ is a viscous coefficient measured in dyn-s/cm^2. The dots on $\dot{\sigma}'_{ij}$ and $\dot{e}'_{ij}$ indicate the time derivatives of the stress and strain deviators, i.e., $\partial\sigma'_{ij}/\partial t$ and $\partial e'_{ij}/\partial t$.

Eqs. 2–7 must be solved subject to the following stress boundary conditions. Let A_G be the area of contact between the glass pipette and the leukocyte (a concentric ring), A_I the area inside the pipette, and A_O the remainder of the cell surface outside the pipette. A schematic drawing of the leukocyte with a micropipette is shown in Fig. 2. Let the pressures acting on these three surfaces of the cell be P_G, P_I, and P_O. Then $\Delta P_I(t) = P_I(t) - P_O$ is the applied suction pressure, which is a function of time in general. P_O is constant and equal to the hydrostatic fluid pressure, which is close to atmospheric pressure, and P_G is computed from the condition of equilibrium for the whole cell expressed in form of surface integrals:

$$\int_{A_O} P_O \nu_i \, dA + \int_{A_G} P_G \nu_i \, dA + \int_{A_I} P_I \nu_i \, dA = 0 \qquad i = 1, 2, 3 \tag{8}$$

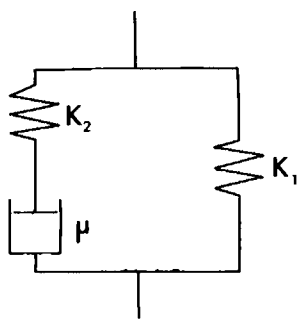

FIGURE 1

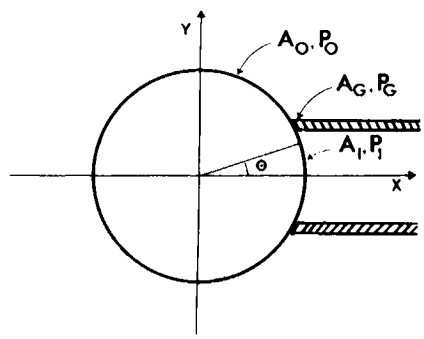

FIGURE 2

FIGURE 1 The standard solid viscoelastic model.

FIGURE 2 Schematic of a leukocyte with micropipette. The areas A_I, A_G and A_O refer to the cell surface inside the pipette, the area of contact with the glass of pipette, and outside area respectively. P_I, P_G, P_O are the corresponding pressures on these surfaces.

where ν_i is the ith component of the unit outer normal vector on the leukocyte. Note that the value of P_G is dependent on A_G, which in turn depends on the wall thickness h_p and radius r_p of the pipette.

The response of a viscoelastic cell is a function of the pressure history $\Delta P_1(t)$. In the experiments a step pressure is applied, which is represented by

$$\Delta P_1(t) = \Delta P\, U(t), \tag{9}$$

where ΔP is the amplitude of the step pressure and $U(t) = 0$ for $t < 0$, and $U(t) = 1$ for $t \geq 0$. The solution for the response of the cell can be obtained by converting the viscoelastic problem into an analogous elastic problem with the aid of a Laplace transform (Fung, 1965). The solution of the elastic problem is known in terms of solid spherical harmonics (Lamb, 1945). An inverse Laplace transform then yields the solution for the specified load history (Eq. 9). We omit here the intermediate steps and give the final result. The displacements at the surface of the sphere with radius a are

$$u_x = a \sum_{n=1}^{\infty} \frac{A_n(t)n}{(2n^2 + 4n + 3)} \left[\frac{3}{2(n-1)} L_{n-1}(\eta) + \eta L_n(\eta) \right], \tag{10a}$$

$$u_y = a \sum_{n=1}^{\infty} \frac{A_n(t)(1-\eta^2)^{1/2}}{(2n^2 + 4n + 3)} \left[n L_n(\eta) - \frac{3}{2(n-1)} L'_{n-1}(\eta) \right], \tag{10b}$$

where $L_n = L_n(\eta)$ are Legendre polynomials that are functions of $\eta = \cos\theta$, where θ is the polar angle (Fig. 2). L'_n is the first derivative with respect to η. The coefficients $A_n(t)$ are the Legendre coefficients of the applied pressure. They are measured in dyn/cm^2 and are computed from the pressure distribution $P(\eta)$ over the surface of the sphere by

$$A_n(t) = J(t) \frac{2n+1}{2} \int_{-1}^{1} P(\eta)\, L_n(\eta)\, d\eta \tag{11}$$

where $J(t)$ is the creep function. For the standard solid model it is

$$J(t) = U(t) \frac{1}{k_1} \left\{ 1 - \left(1 - \frac{k_1}{k_1 + k_2} \right) \exp\left[- \frac{k_1 k_2}{(k_1 + k_2)\mu} t \right] \right\}. \tag{12}$$

Note that the coefficients $A_n(t)$ are dependent on the dimensions of the white cell and on the wall thickness and radius of the micropipette.

EXPERIMENTAL METHODS

Cell Preparation

Fresh blood samples (20–30 ml) were obtained from the medial antecubital vein of several laboratory personnel volunteers (age 22–29 yr) with EDTA as the anticoagulant. The erythrocytes were allowed to sediment at room temperature for 25–40 min. The supernatant plasma layer containing the leukocytes, platelets, and a few erythrocytes were collected with a Pasteur pipette and suspended in a saline solution containing 0.1 g/100 ml EDTA, 0.25 g/100 ml serum albumin, with the pH adjusted to 7.4 by the dropwise addition of HCl. The final concentration of leukocytes was ~50 cells/mm^3. The prepared cells were studied ~45 min after phlebotomy, and the experiment was completed after about 4 h.

Instrumentation

The microscope and micropressure system is the same as that used for the experiments with erythrocytes (Chien et al., 1978). About 1–2 ml of the cell suspension was placed in a small round chamber which was mounted on the stage of an inverted microscope. Individual cells were viewed through the bottom of the chamber with a ×100 objective (NA 1.24, oil immersion) and a ×20 eyepiece. The image was recorded with the use of a video camera, stored on a video tape recorder system, and displayed on a monitor. The magnification was calibrated with the use of a microscale (50 × 2 μm, Graticules Ltd., Towbridge, Kent, England), and the time was recorded with a video timer.

Micropipettes with internal radius between 1.1 and 1.8 μm were prepared with a micropipette puller

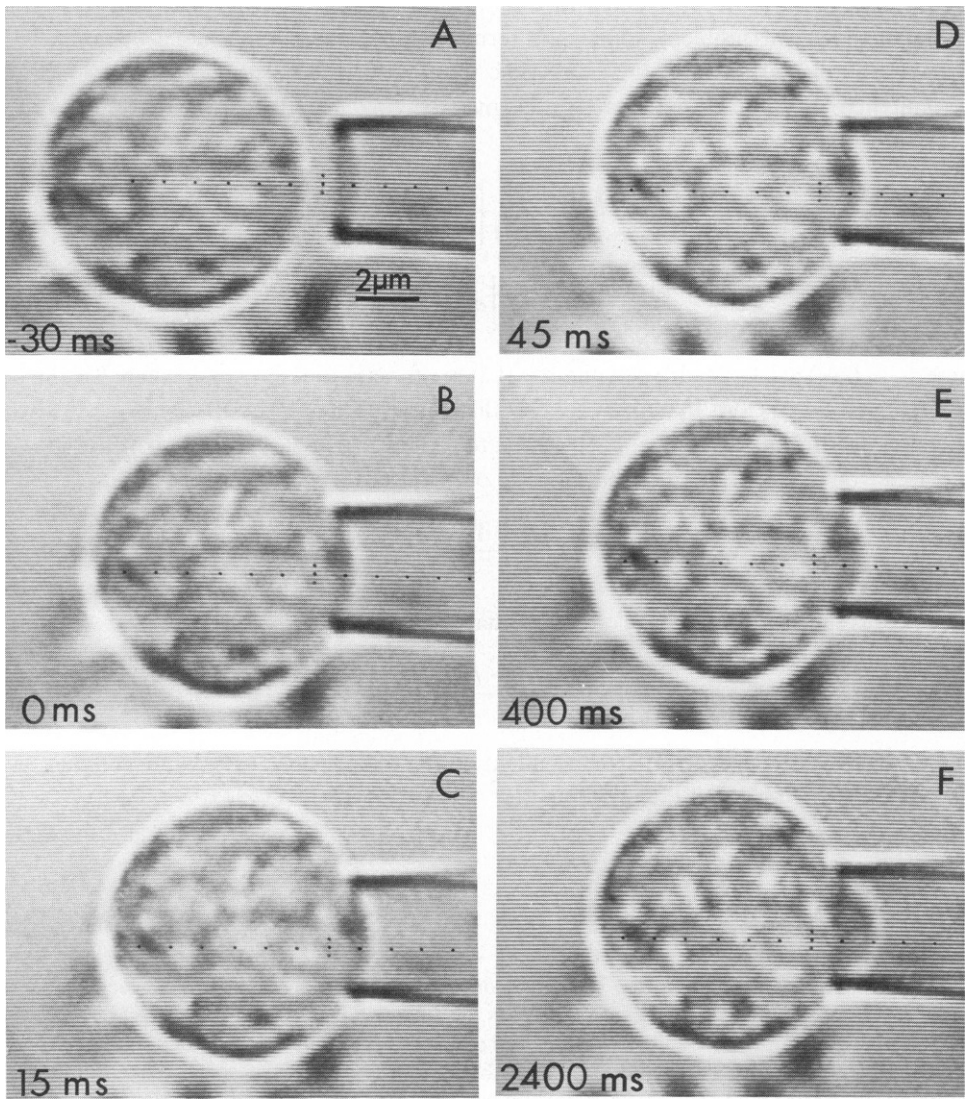

FIGURE 3 Sequence of photographs showing the progressive deformation of the cell at the indicated times after the cell made contact with the pipette. The applied pressure amplitude ΔP = 500 dyn/cm^2. The cell is suspended in a medium of 310 mosmol and 22°C.

and filled with the same salt solution in which the cells were suspended. The micropipette was mounted on a micromanipulator and connected to a pressure regulator (for details see Chien et al., 1978). With this pressure regulator it is possible to suddenly apply an aspiration pressure via the micropipette. For an aspiration pressure of -200 mm H_2O the time interval to reach full amplitude is ~30–40 ms.

Protocol and Data Reduction

The micropipette was positioned adjacent to the leukocyte. When the aspiration pressure was applied, the leukocyte was drawn towards the pipette tip together with some fluid that entered the pipette. At the moment the leukocyte sealed the pipette, this fluid motion stopped, as could be seen from the displacement of adjacent platelets inside or outside of the micropipette.

At the moment when the leukocyte made contact with the micropipette it deformed. This deformation was recorded on the video system, and all measurements were obtained from photographic records of the television monitor made during single frame replay, as shown in Fig. 3. The time between single frames is ~16 ms. The displacement of the cell surface into the pipette was measured to the outer edge of the dark interference band of the cell. As shown in Fig. 4 *c*, if $l(t)$ is the distance from the tip of the pipette to the tip of the leukocyte tongue inside the pipette, and d_0 the height of the spherical cap of the undeformed cell (Fig. 4 *b*), then $d(t) = l(t) - d_0$ is the extent of the deformation of the leukocyte tongue into the pipette. But $d(t)$ is also equal to the sum of the displacements $u_x^A(t)$ at point A and $u_x^B(t)$ at point B. Thus, $d(t) = |u_x^A(t)| + |u_x^B(t)|$ (Fig. 4 *a*). This figure shows the shape of the cell computed according to Eq. 10.

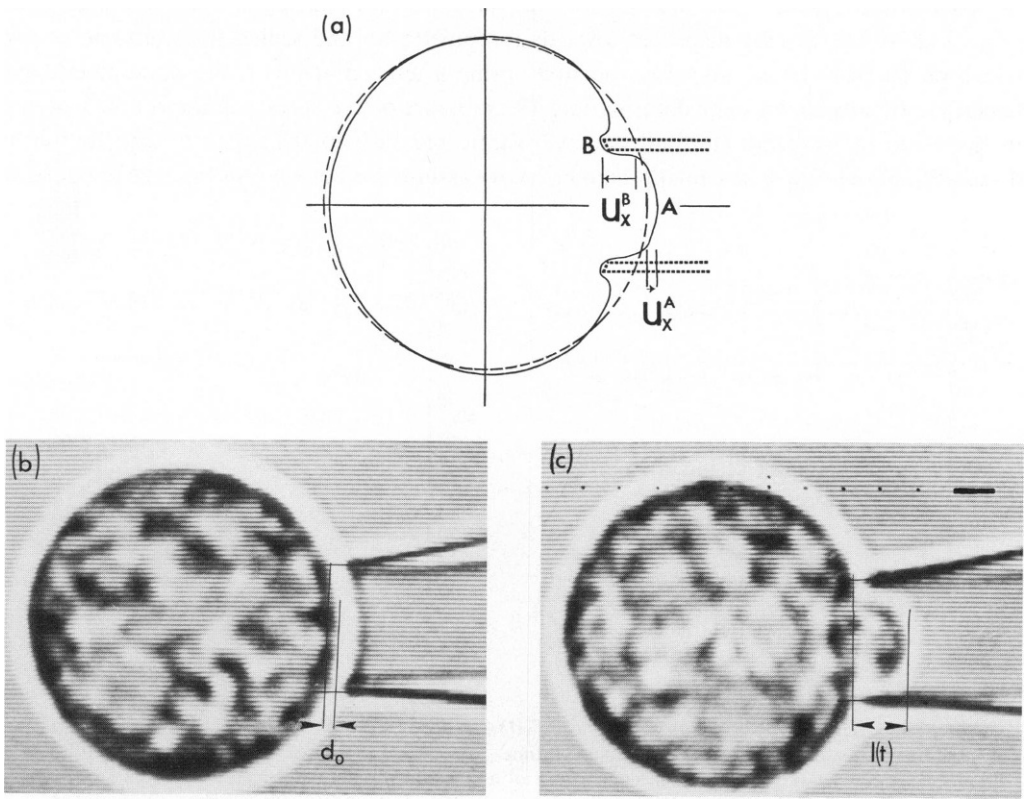

FIGURE 4 The shape of the deformed cell. (*a*) Computed shape and (*b*,*c*) actual shape for a cell with equal diameter and pipette size as in *a*. The displacements $d'(t)$ and $d(t)$ are computed and measured as indicated in the text. Note that the entire cell deforms in this experiment.

To determine the viscoelastic coefficients k_1, k_2, and μ that best fit the experimental results, the following procedure was used. Let $d_1, d_2, \ldots, d_n$ be the measured surface displacements into the pipette at the times $t_1, t_2, \ldots, t_n$ and let $d'(t_1), d'(t_2), \ldots, d'(t_n)$ be the computed displacements for the same cell diameter, pipette radius, and wall thickness. Consider the error measure ϵ defined by

$$\epsilon(k_1, k_2, \mu) = \sum_{k=1}^{n} | d_k - d'(t_k) |^2. \tag{13}$$

The best fit of the viscoelastic model to the experimental data is obtained when ϵ assumes a minimum. A necessary condition is

$$\frac{\delta\epsilon}{\delta k_1} = \frac{\delta\epsilon}{\delta k_2} = \frac{\delta\epsilon}{\delta\mu} = 0. \tag{14}$$

Eq. 14 leads to three equations for the three unknown viscoelastic coefficients which, owing to the presence of transcendential functions, have to be solved by an iterative algorithm. This computation and the computation of the cell shape according to Eqs. 10–12 were implemented on a PDP 11/10 minicomputer (Digital Equipment Corp., Maynard, Mass.).

RESULTS

Fig. 5 shows the pressure and displacement histories for a single experiment. At the moment the aspiration pressure in the micropipette was turned on, the neutrophil was still undeformed (Fig. 3 *a*). It was rapidly displaced towards the pipette tip and sealed it within one or two television frames (16–32 ms). On the first frame after contact with the micropipette the leukocyte already shows some deformation. The pressure on the surface of the cell was altered in the same period from the uniform hydrostatic pressure to the pressure distribution as discussed above in Eq. 8. As an approximation, we assume for the analysis that the pressure on

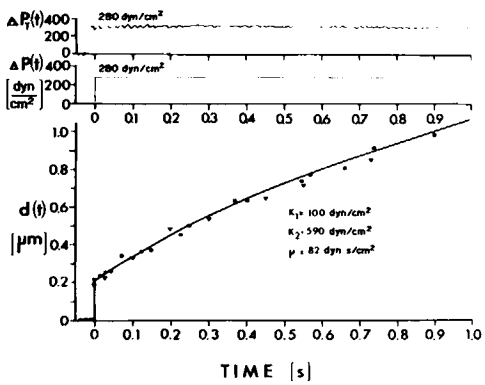

FIGURE 5

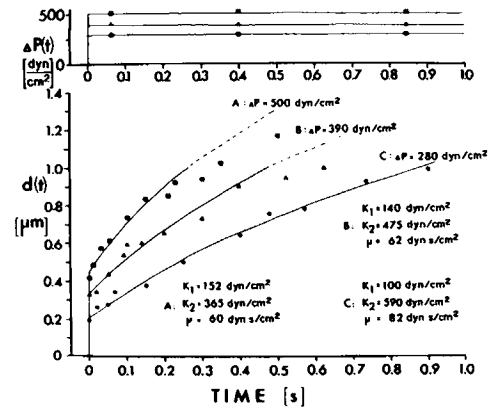

FIGURE 6

FIGURE 5 The recorded transducer pressure $\Delta P_T(t)$, the pressure on the surface of the leukocyte $\Delta P(t)$ and the displacement $d(t)$ as a function of time. The different symbols (●, ▼, ■) represent the displacement measured at three different points of a single neutrophil suspended in a medium of 310 mosmol at 22°C. The solid curve is the theoretical result using the best-fit coefficients k_1, k_2, and μ listed.

FIGURE 6 The aspiration pressure $\Delta P(t)$ and displacement $d(t)$ for three different amplitudes of $\Delta P(t)$ on a single neutrophil. For displacements $<\sim 1$ μm, the values of $d(t)$ are proportional to the applied pressure amplitude. The cell was suspended in the same medium as in Fig. 5.

the surface of the leukocyte was changed stepwise at time $t = 0$. After the initial deformation, which is considered to be an elastic response, the cell surface shows a creep displacement that is nonlinear with time. The continuous line for $d(t)$ in Fig. 5 represents the best possible fit of the standard solid model to the experimental data. The best-fit coefficients k_1, k_2, and μ are listed in Fig. 5. The different symbols for $d(t)$ in Fig. 5 represent three experiments measured at different points on the surface of the same neutrophil. This was achieved by rotating the cell after each experiment. The close agreement of the three experiments suggests that the cell has relatively homogeneous mechanical properties. Similar results were obtained for other neutrophils, monocytes, and esosinophils.

In general, although leukocytes can undergo large deformation, the current continuum

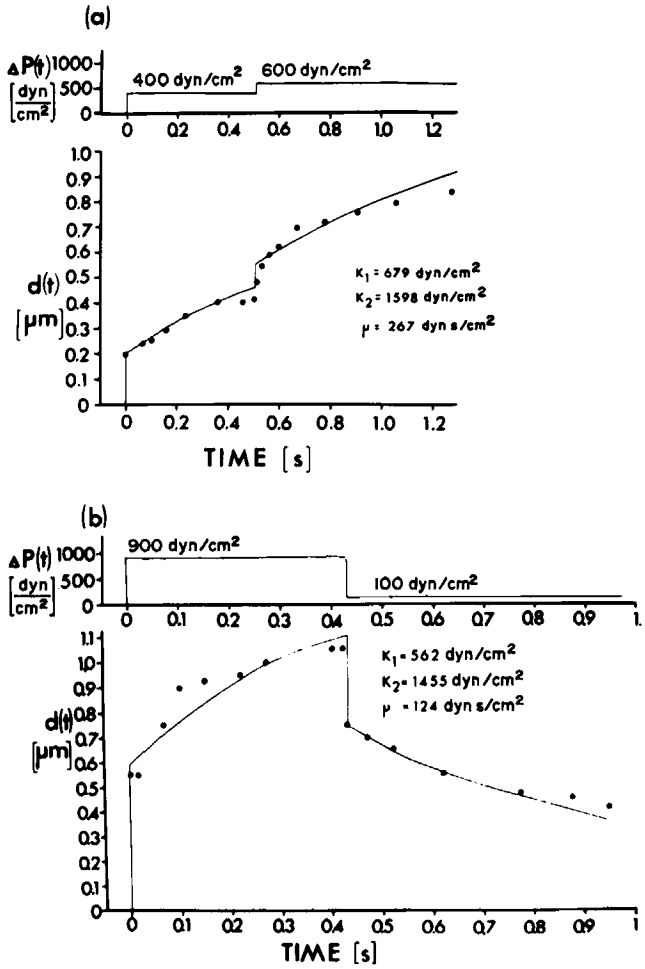

FIGURE 7 The aspiration pressure $\Delta P(t)$ and displacement $d(t)$ for a two-step loading experiment (*a*) and for a loading-unloading experiment (*b*). The coefficients were computed only from values of $d(t)$ obtained before the second step loading (*a*) or before the unloading (*b*). The lines drawn for the second step loading (*a*) and unloading (*b*) represent predictions without changes of the value of k_1, k_2, and μ. The neutrophils were suspended in the same medium as in Fig. 5.

mechanical model assumes that the strains are small and that there exists a linear relation between the strain and the displacements (Eq. 2). Therefore, the solution (Eq. 10) may be written in the abbreviated form

$$d'(t) = J(t)\Delta P f(a, r_p, h_p). \tag{15}$$

In other words, there exists at any instant a linear relation between the displacement $d'(t)$ and the pressure amplitude ΔP. This assumption can be tested experimentally. Fig. 6 shows that for deformations $d(t)$ that are $<\sim 10\%$ of the cell diameter, this assumption is closely satisfied. For larger deformations, however, the model overestimates the experimental results.

Another way to test the assumption of linearity as well as the validity of the standard solid model is to apply, after the first pressure step at $t = 0$, a second step at $t = t_0 > 0$ with an additional aspiration pressure. Fig. 7 shows the results of such experiments. The coefficients k_1, k_2, and μ were computed only for the first step (for $t < 510$ ms in Fig. 7 *a* and $t < 420$ ms in Fig. 7 *b*). The theoretical line drawn for the second step represents a prediction based on the coefficients derived from the results obtained from the first step. We find that as long as the deformation during the second step remains within the linear region ($<\sim 0.8$ μm) the prediction is satisfactory, but beyond this point the model generally overestimates the measured displacements.

Studies on 75 neutrophils suspended in isotonic buffer (310 mosmol and pH 7.4) at a temperature of 22°C have generated the following coefficients (mean ± SD): $k_1 = 275 \pm 119$ dyn/cm^2, $k_2 = 737 \pm 346$ dyn/cm^2, and $\mu = 130 \pm 54$ dyn-s/cm^2. The values for monocytes and eosinophils fall into the same range.

DISCUSSION

Cell Homogeneity

The cytoplasm of human leukocytes is morphologically heterogeneous (Schmid-Schönbein et al., 1980*b*). However, when leukocytes are aspirated at different locations on their surface with the same pipette and constant pressure amplitude, one obtains a remarkably similar deformation history, which suggests relatively homogeneous elastic properties on the scale of the micropipette test (Fig. 5). Therefore, the major part of the scatter in experimental results is attributable to variations among individual leukocytes due to treatment, age, uncertainty in the measurements (e.g., pipette geometry; see Appendix on Error Analysis), and other factors.

Rheological Model

In a series of pilot experiments with pipette diameters of ~ 1 μm i.d. the initial elastic deformation at $t = 0$ was small and could not be observed in all cases. But with larger pipettes (2–3 μm i.d.) this deformation is regularly visible.

The standard solid model is the simplest viscoelastic model that fits the experimental results. For small strains the agreement is close, but for large deformations, i.e., $d(t) > 0.9$ μm, the computed surface displacements overestimate the measured values. This is to be expected because (*a*) the assumption of a small displacement gradient underlying Eq. 2 is no longer accurate, and (*b*) the cell membrane may contribute to the deformation response. After

the membrane of the portion of the cell inside the pipette has been unfolded, further deformation would necessitate the sliding of additional membrane across the contact area with the glass (A_G), which may cause an additional frictional stress. Then the normal stress boundary condition (Eq. 8) may not be accurate anymore. From the measurements of the excess membrane area σ (Schmid-Schönbein et al., 1980*b*), one can estimate the critical displacement d_{crit} at which the membrane inside the pipette would be unfolded without drawing additional membrane into the pipette. Assuming a spherical cap shape for the cell tongue, one finds $d_{crit} = 1.1$ μm at a typical $\sigma = 80\%$ for neutrophils. As noted above, for $d(t) > 0.9$ μm, measured displacements are generally below the values predicted by the model.

The finding of viscoelastic properties for human neutrophils is in qualitative agreement with the results by Bagge et al., (1977), in whose study the deformation and recovery characteristics of normal granulocytes in a capillary tube with stenosis was also fitted by a standard solid model. Bagge et al., however, assumed a simplified one-dimensional deformation field, so that no quantitative comparison of their viscoelastic coefficients can be made directly with the results in this report.

It is of interest to express the elastic response of the cell also in the form of a shear modulus G as it is used in Hooke's law (Fung, 1965). For an infinitely slow motion $G = k_1/2$ is ~130 dyn/cm^2, and for infinitely fast motion $G = (k_1 + k_2)/2$ is ~506 dyn/cm^2.

Adhesion to the Micropipette

It may be suggested that our results are biased because of adhesion of the cell to the micropipette. It often happens that, after the cell has been aspirated into the pipette and the aspiration pressure ΔP is returned to zero, the cell does not slide freely out of the pipette but adheres at one or more points to the glass. This happens frequently when a large tongue is aspirated into the pipette with $d(t) > 1$ μm. In such cases a positive pressure is needed to remove the cell, which indicates that an adhesive force exists between cell membrane and the glass. In this study, all such records were discarded, and only those were retained where the cell slides freely out of the pipette after the removal of the aspiration pressure without any application of positive pressure. There may also be some friction between the cell membrane and glass without adhesion. For small deformations, however, the membrane reacts mostly by unfolding, and no membrane has to slide across the contact area A_G. Therefore, the influence of friction is assumed to be negligible.

Cell Membrane Properties

In the current model the cell is regarded as a solid sphere, and no separate evaluation was made on the contributions of cell membrane and cytoplasm. Thus, the viscoelastic coefficients reflect the properties of the entire cell. The results in hypoosmotically swollen cells, however (Sung et al., 1981), suggest that the cell membrane has a relatively large area extensibility modulus which is similar to that seen in the erythrocyte membrane (Evans et al., 1976; Evans and Waugh, 1977). This is in agreement with our direct morphometric measurements (Schmid-Schönbein et al., 1980*b*) that show constant area of the cellular, nuclear, granular, and mitochondria membranes during swelling.

Further Improvements

Several simplifying assumptions were made in this study, which should be relaxed in future work. The assumption of a step-pressure increase neglects the gradual rise of the surface stress as the cell approaches the pipette tip. The details of the pipette geometry (such as the plane edge at the tip) should be introduced in the model, and the geometry of the pipette tip should be studied closely in the experiments, possibly with scanning electron microscopy. Finally, the assumption of homogeneous mechanical properties should be replaced by a heterogeneous model with cell nucleus, granules, and membrane, and the surface foldings should be treated separately in the model.

Previous Leukocyte Micropipette Experiments

Lichtman (1973) and Miller and Myers (1975) have applied micropipette suction to study human leukocytes, but their experiment is designed differently from ours. They used pipettes with larger inner diameter (~5 μm) to pull the entire cell inside the pipette and used the pressure needed for this process as a measure of the elasticity of the cell. Since (*a*) the overall cell geometry is an important factor in these studies, and (*b*) there may be an adhesive force between the tightly fitting cell and the inner wall of the pipette, when there is a large contact area between cell and glass, their experiments may not be interpretable in terms of cell elastic properties alone.

Physiological Implications

The coefficients of viscosity μ of leukocytes under normal physiological conditions are ~130 poise. This is ~2,000 times higher than the viscosity of the hemoglobin solution inside the erythrocyte. In addition, the leukocytes have about twice the volume of erythrocytes (Schmid-Schönbein et al., 1980*b*). Therefore, leukocytes impose a much larger resistance in capillary blood vessels than erythrocytes (Bagge et al., 1977). Under the condition of hypotension in the circulation this may lead to plugging of leukocytes at the entrance to capillary vessels and thus to cessation of flow (Bagge et al., 1980). Owing to the lower velocity of leukocytes than that of erythrocytes in capillaries, a hydrodynamic collision follows which leads to regular attachment of leukocytes on the venous endothelium (Schmid-Schönbein et al., 1980*a*). The relatively small deformation of the leukocytes on the venous endothelium (Schmid-Schönbein et al., 1975) with a major portion of the cell reaching into the flow field in venules causes a large elevation of the flow resistance in these vessels (Lipowsky et al., 1980).

The viscoelastic behavior and the geometric factors (almost constant membrane area) of leukocytes are of fundamental importance in the understanding of their interaction with the endothelium, and the analysis of their migration, phagocytosis, or any other function. The constant membrane area forms a boundary condition that any detailed analysis of such motions must satisfy.

APPENDIX

Error Analysis

An estimate of the error in the measurement of k_1, k_2, and μ can be obtained in the following way. Each coefficient is a function of the five measured variables: The diameter of the cell d_c, the diameter d_p and wall thickness h_p of the pipette, the suction pressure P_1, and the displacement $d(t)$. Consider for example

TABLE IA
RESULTS OF ERROR ANALYSIS

$\left\lvert\frac{\partial k_1}{\partial d_c}\right\rvert \frac{\delta d_c}{k_1} = 0.107$	$\left\lvert\frac{\partial k_2}{\partial d_c}\right\rvert \frac{\delta d_c}{k_2} = 0.139$	$\left\lvert\frac{\partial \mu}{\partial d_c}\right\rvert \frac{\delta d_c}{\mu} = 0.171$
$\left\lvert\frac{\partial k_1}{\partial d_p}\right\rvert \frac{\delta d_p}{k_1} = 0.357$	$\left\lvert\frac{\partial k_2}{\partial d_p}\right\rvert \frac{\delta d_p}{k_2} = 0.503$	$\left\lvert\frac{\partial \mu}{\partial d_p}\right\rvert \frac{\delta d_p}{\mu} = 0.326$
$\left\lvert\frac{\partial k_1}{\partial h_p}\right\rvert \frac{\delta h_p}{k_1} = 0.059$	$\left\lvert\frac{\partial k_2}{\partial h_p}\right\rvert \frac{\delta h_p}{k_2} = 0.503$	$\left\lvert\frac{\partial \mu}{\partial h_p}\right\rvert \frac{\delta h_p}{\mu} = 0.652$
$\left\lvert\frac{\partial k_1}{\partial P_1}\right\rvert \frac{\delta P_1}{k_1} = 0.084$	$\left\lvert\frac{\partial k_2}{\partial P_1}\right\rvert \frac{\delta P_1}{k_2} = 0.008$	$\left\lvert\frac{\partial \mu}{\partial P_1}\right\rvert \frac{\delta P_1}{\mu} = 0.065$
$\left\lvert\frac{\partial k_1}{\partial d}\right\rvert \frac{\delta d}{k_1} = 0.178$	$\left\lvert\frac{\partial k_2}{\partial d}\right\rvert \frac{\delta d}{k_2} = 2.108$	$\left\lvert\frac{\partial \mu}{\partial d}\right\rvert \frac{\delta d}{\mu} = 0.271$

Mean values: $k_1 = 56$ dyn/cm^2, $k_2 = 596$ dyn/cm^2, $\mu = 92$ dyn-s/cm^2, $d_c = 8.5$ μm, $d_p = 3.5$ μm, $h_p = 0.3$ μm.

the elastic coefficient

$$k_1 = k_1 (d_c, d_p, h_p, P_1, d). \tag{A1}$$

Each measured quantity has an uncertainty δd_c, δd_p, δh_p, δP_1, and δd. The magnitude of the uncertainty of the elastic coefficient δk_1 can be evaluated by taking the total differential in Eq. A1. The maximum relative error $\delta k_1/k_1$ with respect to a typical value k_1 is

$$\frac{\delta k_1}{k_1} = \left\lvert\frac{\partial k_1}{\partial d_c}\right\rvert \frac{\delta d_c}{k_1} + \left\lvert\frac{\partial k_1}{\partial d_p}\right\rvert \frac{\delta d_p}{k_1} + \left\lvert\frac{\partial k_1}{\partial h_p}\right\rvert \frac{\delta h_p}{k_1} + \left\lvert\frac{\partial k_1}{\partial P_1}\right\rvert \frac{\delta P_1}{k_1} + \left\lvert\frac{\partial k_1}{\partial d}\right\rvert \frac{\delta d}{k_1}. \tag{A3}$$

A similar equation exists for k_2 and μ. The partial differentials $\partial k_1/\partial d_c$ etc. can be estimated from the solution (Eq. 10) by repeating the computation of k_1 according to Eqs. 13 and 14, and by parametrically altering each measured quantity above and below its mean value. The results of this computation are given in Table IA. It is assumed that $\delta d_c = \delta h_p = \delta d_p = \delta d = 0.2$ μm, $\delta P_1 = 20$ dyn/cm^2. Adding the individual terms in Table IA, we find $\delta k_1/k_1 = 0.785$, $\delta k_2/k_2 = 3.261$, and $\delta\mu/\mu = 1.485$. This is the maximum error to be expected. It is interesting to note that, as shown in Table IA, an uncertainty in the needle geometry introduces a major error in the measurement of the elastic coefficient. Thus a verification of the values of d_p and h_p by scanning electron microscopy reduces the error significantly. We have made such a comparison and have found that the light microscopic estimate of d_p and h_p agrees within 0.1 μm with the scanning electron microscopy measurement.

Received for publication 24 February 1981 and in revised form 5 June 1981.

REFERENCES

Bagge, U., and P.-I. Brånemark. 1977. White blood cell rheology. An intravital study in man. *Adv. Microcirc.* 7:1–17.

Bagge, U., R. Skalak, and R. Attefors. 1977. Granulocyte rheology. Experimental studies in an in vitro microflow system. *Adv. Microcirc.* 7:29–48.

Bagge, U., B. Amundson, and C. Lauritzen. 1980. White blood cell deformability and plugging of skeletal muscle capillaries in hemorrhagic shock. *Acta Physiol. Scand.* 180:159–163.

Chien, S. 1977. Principles and techniques for assessing erythrocyte deformation. *Blood Cells.* 3:71–99.

Chien, S., K. L. P. Sung, R. Skalak, S. Usami, and A. Tözeren. 1978. Theoretical and experimental studies on viscoelastic properties of erythrocyte membrane. *Biophys. J.* 24:463–487.

Elsbach, P. 1974. Phagocytosis. *In* The Inflammatory Process. B. W. Zweifach, L. Grant, and R. T. McCluskey, editors. Academic Press Inc., New York. 2nd edition. 1:363–410.

Evans, E. A. 1973. New membrane concept applied to the analysis of fluid shear- and micropipette-deformed red blood cells. *Biophys. J.* 13:941–954.

Evans, E. A., R. Waugh, and L. Melnik. 1976. Elastic area compressibility modulus of the red cell membrane. *Biophys. J.* 16:585–595.

Evans, E. A., and R. Waugh. 1977. Osmotic correction to elastic area compressibility measurements on red cell membrane. *Biophys. J.* 20:307–313.

Evans, E. A., and R. M. Hochmuth. 1978. Mechanochemical properties of membranes. *Curr. Top. Membr. Transp.* 10:1–64.

Fung, Y.-C. 1965. Foundations of solid mechanics. Prentice-Hall, Inc., Englewood Cliffs, N.J.

Gallin, J. I., and P. C. Quie, editors. 1978. Leukocyte Chemotaxis: Methods, Physiology and Clinical Implications. Raven Press, New York.

LaCelle, P. L., E. A. Evans, and R. M. Hochmuth. 1977. Erythrocyte elasticity, fragmentation and lysis. *Blood Cells.* 3:335–350.

Lamb, H. 1945. Hydrodynamics. 6th edition. Dover Publications, Inc., New York.

Lichtman, M. A. 1973. Rheology of leukocytes, leukocyte suspensions, and blood in leukemia. *J. Clin. Invest.* 52:350–358.

Lipowsky, H. H., S. Usami, and S. Chien. 1980. In vivo measurements of "apparent viscosity" and microvessel hematocrit in the mesentery of the cat. *Microvasc. Res.* 19:297–319.

Miller, M. E., and K. A. Myers. 1975. Cellular deformability of the human peripheral blood polymorphonuclear leukocyte: Method of study, normal variation, effects of physical and chemical alterations. *Res. J. Reticuloendothel. Soc.* 18:337–345.

Rand, R. P., and A. C. Burton. 1964. Mechanical properties of the red cell membrane. I. Membrane stiffness and intracellular pressure. *Biophys. J.* 4:115–135.

Schmid-Schönbein, G. W., Y.-C. Fung, and B. W. Zweifach. 1975. Vascular endothelium-leukocyte interaction: sticking shear force in venules. *Circ. Res.* 36:173–184.

Schmid-Schönbein, G. W., S. Usami, R. Skalak, and S. Chien. 1980*a*. The interaction of leukocytes and erythrocytes in capillary and postcapillary vessels. *Microvasc. Res.* 19:45–70.

Schmid-Schönbein, G. W., Y. Y. Shih, and S. Chien. 1980*b*. Morphometry of human leukocytes. *Blood.* 56:866–875.

Schmid-Schönbein, G. W., K. L. P. Sung, and S. Chien. 1981. Human leukocytes in the passive and active state. *Microvasc. Res.* 21:256A.

Sung, K. L. P., G. W. Schmid-Schönbein, R. Skalak, G. B. Schuessler, S. Usami, and S. Chien. 1981. Influence of physiocochemical factors on rheology of human neutrophils. *Blood.* In review.

Tözeren, H., and R. Skalak. 1978. The steady flow of closely fitting incompressible elastic spheres in a tube. *J. Fluid Mech.* 87:1–16.